Numerical Modeling of Seismic Response of Rigid Foundation on Soft Soil

M. H. T. Rayhani, Ph.D., S.M.ASCE[1]; and M. H. El Naggar, M.ASCE[2]

Abstract: A numerical model was developed to simulate the response of two instrumented, centrifuge model tests on soft clay and to investigate the factors that affect the seismic ground response. The centrifuge tests simulated the behavior of a rectangular building on 30 m uniform and layered soft soils. Each test model was subjected to several earthquakelike shaking events at a centrifugal acceleration level of 80*g*. The applied loading involved scaled versions of an artificial western Canada earthquake and the Port Island ground motion recorded during the 1995 Kobe Earthquake. The centrifuge model was simulated with the three-dimensional finite-difference-based fast Lagrangian analysis of continua program. The results predicted with the use of nonlinear elastic–plastic model for the soil are shown to be in good agreement with measured acceleration, soil response, and structural behavior. The validated model was used to study the effect of soil layering, depth, soil–structure interaction, and embedment effects on foundation motion.

DOI: 10.1061/(ASCE)1532-3641(2008)8:6(336)

CE Database subject headings: Numerical models; Centrifuge models; Soft soils; Soil-structure interaction; Foundations.

Introduction

The use of model tests in geotechnical engineering offers the advantage of simulating complex systems under controlled conditions, and the opportunity to gain insight into the fundamental mechanisms operating in these systems. Model test results are often used as calibration benchmarks for analytical methods, or to make quantitative predictions of the prototype response. Such models, when subjected to a controlled base motion, can also provide a database for the validation of numerical approaches. However, soil behavior is highly stress dependent, and thus small models under a 1*g* acceleration field are not representative of field conditions. On the other hand, centrifuge tests that utilize a high acceleration field can replicate the stress–strain response of the prototype soil and can give a realistic representation of field behavior.

The effects of soil–structure interaction (SSI) and nonlinear site response (SR) were the focus of several studies. Veletsos and Prasad (1989) and Balendra and Heidebrecht (1986) showed that SSI effects are significant only for short-period structures. However, such effects may be important for medium- and long-period structures when the predominant site period is large. Aviles and Perez-Rocha (1997) investigated site effects and SSI during the Mexico earthquake of 1985. Based on their study, significant effects of SSI have been identified for medium- and long-period structures founded on soft soils. Interaction effects were found to be larger for tall and slender structures than for short and squat structures of the same period, and they decreased as the foundation depth increased.

Soil–structure interaction may produce either amplification or reduction of the base shear, depending on the spectral period at which the response spectra with and without interaction cross each other. The SSI can affect the base shear demand through two distinct mechanisms: inertial interaction and kinematic interaction. Kinematic interaction effects reduce the amplitude of foundation motions relative to the free field due to the differences in stiffness between the foundation and surrounding soil, mainly as a result of base slab averaging, embedment effects, and wave scattering (e.g., Luco and Mita 1987; Veletsos and Prasad 1989; Elsabee and Morray 1977). These effects are most pronounced at high frequencies (short periods) of excitation (Luco and Wong 1986; Veletsos et al. 1997). Stewart et al. (2003) indicated that for stiff structures founded on soil, such as shear wall or braced frame lateral load resisting systems with small aspect ratios, the effects of SSI were found to be most significant. For long-period structures, e.g., high-rise buildings, the effects of SSI are found to be negligible because of the large structure flexibility. Kim and Roesset (2004) studied the effect of nonlinear soil behavior on the inelastic seismic response of structures. They considered structures with variable height, modeled as equivalent linear or nonlinear single degree of freedom systems. The soil nonlinearity was modeled using a finite-element model and an approximate linear iterative procedure. The results demonstrated the importance of accounting for nonlinear soil behavior on the response of structures and that SSI effects are negligible for flexible structures on stiff soils, but are important for stiff structures on soft soils.

Crouse and Ramirez (2003) investigated SSI and SR using the main shock and aftershock motions of the 1994 Northridge Earthquake recorded at two buildings in the Jensen Filtration Plant. Nonlinear SR and kinematic SSI were identified as the main reasons for the differences observed in three sets of the building earthquake records. Each set had clearly distinct amplitude and

[1]Associate Research Director, GeoEngineering Centre, Dept. of Civil Engineering, Queen's Univ., Kingston, ON, Canada K7L 3N6; formerly, Dept. of Civil and Environmental Engineering, Univ. of Western Ontario, London ON, Canada N6A 5B9 (corresponding author). E-mail: mrayhani@ce.queensu.ca

[2]Professor, Dept. of Civil and Environmental Engineering, Univ. of Western Ontario, London ON, Canada N6A 5B9. E-mail: helnaggar@eng.uwo.ca

Note. Discussion open until May 1, 2009. Separate discussions must be submitted for individual papers. The manuscript for this paper was submitted for review and possible publication on March 12, 2007; approved on March 20, 2008. This paper is part of the ***International Journal of Geomechanics***, Vol. 8, No. 6, December 1, 2008. ©ASCE, ISSN 1532-3641/2008/6-336–346/$25.00.

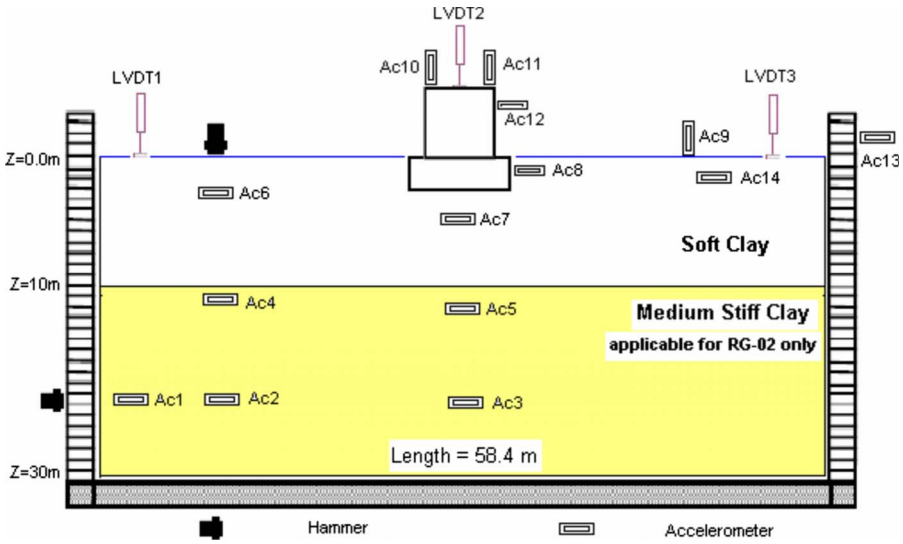

Fig. 1. Centrifuge model configuration in prototype scale

duration characteristics. Borja et al. (1999) developed a three-dimensional (3D) finite-element model to study SSI effects on the response of the Large-Scale Seismic Test site in Lotung, Taiwan, during the earthquake of May 20, 1986. They considered the response of a 1/4-scale nuclear plant containment structure. Based on this analysis, SSI effects were shown to be partly responsible for the reduced peak north-south ground surface acceleration recorded by a down-hole array near the containment structure. However, models of inertial SSI, calibrated to vibration test data, demonstrated that this phenomenon was of secondary importance, even when adjusted for nonlinear behavior of the soil and structure (Crouse and Ramirez 2003).

Scale model tests have been successfully calibrated against prototype test results, demonstrating the viability of the scaled modeling technique. However, scaled physical models are sensitive to container boundary effects, scale modeling techniques, and adherence to similitude laws. Many aspects of soil–structure interaction have been studied using scale modeling especially centrifuge tests including: effect of foundation rocking on the behavior of soil–foundation system (Faccioli et al. 2001; Georgiadis and Butterfield 1988; Wiessing 1979); effect of foundation size, shape, and embedment depth on foundation response in centrifuge (Hushmand 1983); nonlinear soil–foundation system response of a rigid shear wall (Gajan et al. 2005); and soil–structure interaction in liquefiable soil (Ghosh and Madabushi 2003).

Field tests were also used to evaluate different aspects of soil–structure interaction for shallow foundations. These studies covered the effect of foundation embedment on the impedance functions (Lin and Jennings 1984); impedance function for flexible and rigid foundations (Luco et al. 1988); the effect of soil heterogeneity on foundation response (DeBarros and Luco 1995); dynamic stiffness and damping for forced vibration and earthquake excitation (Kim 2001); and procedures for SSI analysis by Kim and Stewart (2003).

The current study examines the effects of SSI and SR on the foundation input motion used for seismic design of structures. A 3D [fast Lagrangian analysis of continua (FLAC), Itasca 2005] numerical model was used to investigate seismic SR and SSI in soft soils. The numerical model was validated/calibrated employing the results of seismic centrifuge tests involving a model foundation in soft soil (Rayhani and El Naggar 2007). The paper presents a brief description of the centrifuge test results and provides the details of the constitutive model and parameters used for the component materials in the model. The validated numerical model was then used to perform a parametric study to examine factors affecting site response, accelerations amplification at different depths, structural behavior, embedment effect, and soil–structure interaction.

Centrifuge Modeling

Centrifuge model tests were conducted at 80g on the C-CORE 5.5 m radius beam centrifuge located at Memorial Univ. of Newfoundland, Canada. An electrohydraulic earthquake simulator was mounted on the centrifuge to apply a one-dimensional prescribed base input motion. A soil container with inner dimensions of 0.73 m in length, 0.3 m in width, and 0.57 m in height was used to contain the model soil. Fig. 1 shows the configurations and instrumentation layout of the model tests.

The system model consisted of a rigid structure box with 5.5 m in length, 2.5 m in width, and 6 m in height and a foundation which embedded about 2 m in the soil bed. The h/r ratio for the building=2.23, where h=hieght of the containment and r=effective radius for an equivalent circular foundation. Such low value of h/r suggests that rocking during seismic shaking is unlikely and horizontal mode of vibration will dominate. The average bearing stress beneath the structure model at 80g was 95 kPa. The total thickness of the soil bed was approximately 0.375 m, simulating 30 m of soil in prototype scale. The models were prepared by tamping the soil in layers to obtain the desired void ratio (90% of maximum dry density).

Glyben clay with glycerin ratios of 45 and 40% were used for the soil models. The resultant variability of each clay layer was checked by conducting vane shear tests at depth and distance intervals of 50 mm in model scale. The density of glyben with 45% glycerin and 55% bentonite was 1,575 kg/m^3 and its voids ratio, e=1.36. The density and void ratio for clay with 40% glycerin were 1,593 kg/m^3 and 1.21.

The models were instrumented to measure free-field and foundation accelerations, free-field displacements, and local displace-

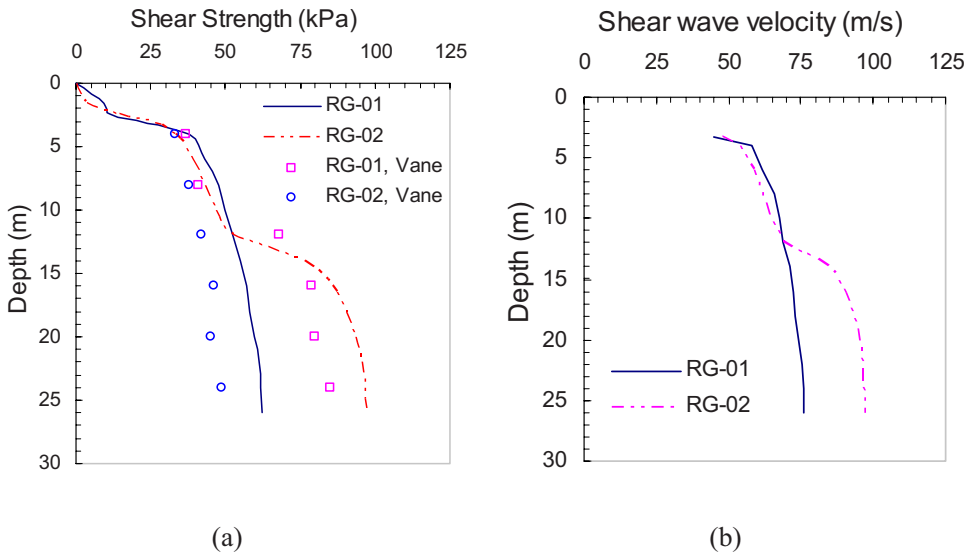

Fig. 2. (a) Shear strength profile; (b) shear wave velocity profile for both models

ment of the basement wall and foundation. Accelerometers were used to measure the soil acceleration at different depths and the structure accelerations. The accelerometers were placed within the soil bed by tamping the clay to the required level, placing the instrument in the desired position, and then adding more soil to the required level. Accelerometers were also placed on top of the structure and on its walls. In addition, the system model was instrumented with linear variable differential transformers to measure the settlement of the soil surface and the vertical displacement of the model structure.

The T-bar test was performed in each clay model at 80g to determine a continuous shear strength profile of the deposit undrained shear strength, S_u. The T-bar results were interpreted using the plasticity solution for the limiting pressure acting on a cylinder moving laterally through purely cohesive soil (Randolph and Houlsby 1984). The analysis assumes full closure of the soil behind the cylinder, such that a gap does not occur. The solution expresses the limiting force acting on an infinitely long cylinder as

$$S_u = P/N_b d \tag{1}$$

where S_u=undrained shear strength; P=force per unit length acting on the cylinder; d=diameter of cylinder, and N_b=bar factor. Randolph and Houlsby (1984) recommended an intermediate value of 10.5 for general use, which has been used to interpret the results. The possible range of N_b is relatively small, and the upper and lower limits correspond to errors of less than $\pm 13\%$ of the adopted value. Fig. 2 shows the soil shear strength profile, determined from T-bar tests. The undrained shear strength measured using the T-bar bearing resistance data varied between 40 and 60 kPa in soft clay (RG-01). The shear strength in Model RG-02 was about 40–50 kPa for upper soft clay and about 85–95 kPa for lower medium stiff clay. The shear strength increased slightly with depth in both models (Rayhani and El Naggar 2007). The shear wave velocity for the lower soil layer was measured using the hammer test, where as the shear wave velocity profile was estimated using established relations between shear strength and shear wave velocity for glyben clay (Rayhani and El Naggar 2008). The estimated shear wave velocity varied between 50 and 90 m/s in RG-01 (soft clay) and between 60 and 130 m/s in Model RG-02 (medium stiff clay). The average shear wave velocity of the 30 m soil profile was about 73 and 100 m/s for Models RG-01 and RG-02, respectively.

Each test model was subjected to several shaking events at a centrifugal acceleration level of 80g, as shown in Table 1. The input excitations were scaled versions of an artificial western Canada earthquake and the Port Island ground motion recorded during the 1995 Kobe Earthquake. The model input motions varied from 2.5g to 43g, at target frequencies from 40 to 200 Hz (simulating prototype earthquakes between 0.03g and 0.54g). The actual patterns of earthquake motion at different level will be shown in Fig. 4. Table 1 also lists peak accelerations at the accelerometer locations: A2 and A3 near the base; A6 near the surface; A7 beneath the structure; and A12 on the structure. The recorded peak acceleration near the model surface ranged from 0.125 to 0.75g. This broad spectrum of acceleration magnitudes resulted in soil response covering linear to nonlinear scenarios. The peak accelerations of the free field appeared to be somewhat less than those beneath the structure.

Numerical Simulation

The numerical analysis is carried out to investigate various factors affecting the seismic response, including the characteristics and

Table 1. Shaking Events and Peak Accelerations (Units in Prototype Scale)

Model	Event ID	Base acceleration (g)	Peak acceleration (g)				
			A2	A3	A6	A7	A12
RG-01	WCL	0.1	0.12	0.125	0.15	0.18	0.2
	WCM	0.18	0.185	0.19	0.24	0.28	0.33
	WCH	0.38	0.375	0.385	0.43	0.51	0.6
	KH	0.54	0.54	0.63	0.61	0.72	0.9
RG-02	WCL	0.1	0.12	0.12	0.19	0.19	0.28
	WCM	0.2	0.21	0.19	0.28	0.275	0.41
	WCH	0.38	0.39	0.39	0.4	0.39	0.49
	KL	0.03	0.04	0.04	0.06	0.06	0.08
	KH	0.54	0.63	0.61	0.61	0.65	0.87

Note: A2–A12=accelerations as shown in Fig. 1.

Table 2. Major Modeling Properties of Soft and Medium Stiff Clay

Model parameters	Soft clay	Medium stiff clay
ρ=mass density (kg/m^3)	1,575	1,595
K=bulk modulus (kPa)	5.7×10^4	9.37×10^4
G=shear modulus (kPa)	8.4×10^3	15.9×10^3
ν=Poisson's ratio (kPa)	0.43	0.42
E=elastic modulus (kPa)	2.4×10^4	4.5×10^4
c=cohesion intercept (kPa)	50	90
ϕ=friction angle (deg)	20	24
c_{sb}=interface cohesion (kPa)	30	50
k_n=normal stiffness (kPa/m)	4.5×10^4	7.6×10^4
k_s=shear stiffness (kPa/m)	5×10^2	8×10^2

depth of soil, the foundation embedment, and soil–structure interaction. The building structure was modeled as a linearly elastic material, whereas the subsoil was modeled as an elastoplastic continuum material that deforms plastically according to the Mohr–Coulomb criteria.

Numerical Approach

The program FLAC3D (Itasca 2005) was used to develop the numerical model for the centrifuge tests and to simulate their response under seismic loading. FLAC3D is a three-dimensional explicit finite-difference program that has the ability to simulate the behavior of soil, rock, or other materials that may undergo plastic flow when their yield limits are reached. The explicit Lagrangian calculation scheme and the mixed-discretization zoning technique used in FLAC3D facilitate accurate modeling of plastic collapse and flow. Materials are represented by elements, and each element behaves according to a prescribed linear or nonlinear stress/strain law in response to the applied forces or boundary restraints.

The Mohr–Coulomb model was used to simulate the nonlinear soil behavior. In FLAC, this model is characterized by its yield function and flow rule. The yield functions define the stress combination for which plastic flow takes place. The model is based on plane strain conditions, and is formulated in terms of effective stresses. The failure envelope corresponds to a Mohr–Coulomb criterion (shear yield) with tension cutoff (tension yield function). The position of a stress point on this envelope is controlled by a nonassociated flow rule for shear failure, and an associated rule for tension failure. The Mohr–Coulomb material model requires conventional soil parameters including: unit weight (γ), friction angle (ϕ), cohesion intercept (c), shear modulus (G), and bulk modulus (B). Table 2 presents the soil parameters used in the FLAC model.

Model Mesh and Boundary Conditions

The soil was modeled with continuum zones, and the structure and its foundation were modeled using structural elements. The foundation was assumed to be rigid (a relatively rigid aluminum foundation was used in the centrifuge tests). Fig. 3 shows the finite-difference grid used in the FLAC model for the soil–structure system. The dimensions of the numerical models were chosen similar to the experimental model. The thickness of the soil bed was 30 m and the total model dimensions were 58.4 m $\times$ 24 m. The mesh size and the maximum unbalanced force at the grid points (i.e., error tolerance) were selected on the basis of a series of parametric analyses to concurrently optimize accuracy and computation speed. The element sizes varied from 0.5 m in each dimension around the building as well as near the surface in the soil to about 2.5 m far from the structure using the wall size technique in FLAC. Numerical computations were carried out in both small- and large-strain modes to ensure sufficient accuracy in the event of weak and strong earthquakes, involving

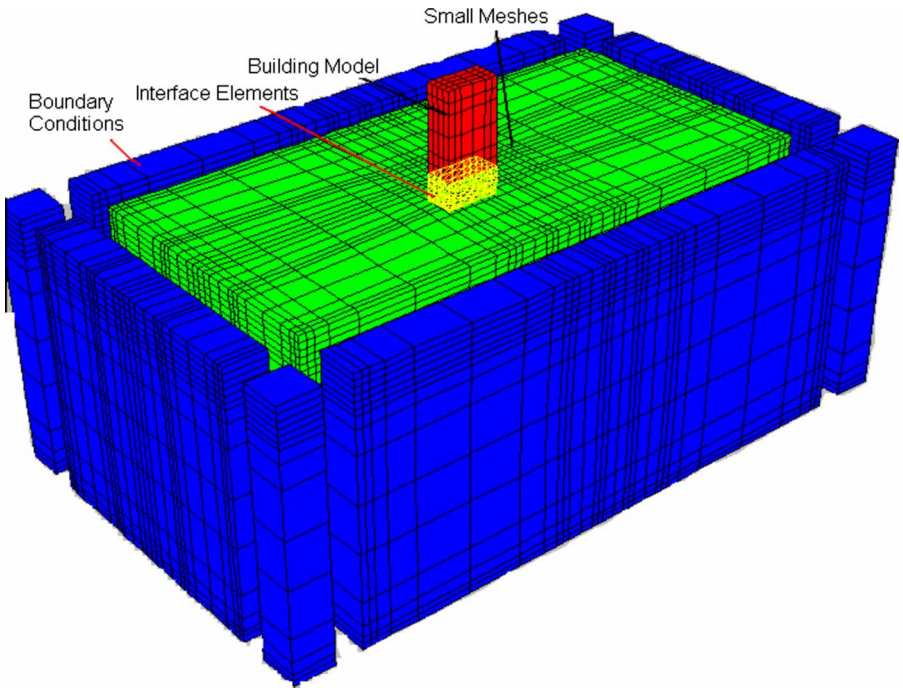

Fig. 3. Numerical grid and model component

small to large deformations. It also accommodated the moving local datum between the foundation and soil layer underneath the foundation.

The boundary conditions in the numerical models consisted of the values of centrifuge test variables (e.g., stress and displacement) that are prescribed at the boundary of the numerical grid. In the static analysis, the soil-structure system was under gravity loading only; the base boundary was fixed in all directions and the side boundaries were fixed in the x and y directions. In the dynamic analysis, the acceleration time history was applied at the entire base horizontally. A fixed condition was assumed at the numerical grid points on the soil side boundaries in the vertical and y directions, representing the centrifuge container that was used to contain the soil in the model tests.

Parameter Identification

The soil was modeled as a nonlinear elastic–plastic material using Mohr–Coulomb failure criterion with nonassociated flow rule. The shear strength values of 50 and 90 kPa were used as representative values for the soft and medium stiff clay soils, respectively. A Poisson's ratio of 0.43 for soft clay and 0.42 for medium stiff clay was employed based on resonant column measurements (Rayhani and El Naggar 2008).

The shaking events presented in Table 1 were applied to the soil model. The analysis was performed with the objective to establish the modeling parameters in order to achieve a satisfactory match between the computed and recorded responses. The dynamic soil properties calculated from the centrifuge test results and verified by the resonant column tests (Rayhani and El Naggar 2008) were used to match the hysteretic damping parameters for nonlinear analysis in FLAC. The damping ratio of glyben was higher than that of natural clays for shear strains below 0.01% (Rayhani and El Naggar 2008). Consequently, Rayleigh damping with an average of 10% was employed in addition to the hysteretic damping generated by the stress–strain model. The adequacy of the matching process was verified by inspecting the recorded and computed shear modulus and damping at all shear strain ranges. Table 2 lists the main model parameters for the soft clay stratum.

The structure and its foundation were modeled using linear elastic elements, with an elastic modulus of 100 GPa and Poisson's ratio of 0.25 and were rigidly connected. The h/r ratio for the structure=3.23, where h=height and r=effective radius for an equivalent circular foundation.

Soil–Foundation Interface

An interface is a connection between subgrids that can separate (e.g., slide or open) during the calculation process. The foundation facing zone in numerical simulations was separated from the adjacent soil zone by interface elements.

The interfaces between the foundation and soil were modeled as linear spring–slider systems, with interface shear strength defined by the Mohr–Coulomb failure criterion. The relative interface movement is controlled by interface stiffness values in the normal (k_n) and tangential (k_s) directions. Based on recommended rule-of-thumb estimates for maximum interface stiffness values given by Itasca Consulting Group (2005), k_n and k_s were set to ten times the equivalent stiffness of the neighboring zone. The apparent stiffness (expressed in stress per distance units) of a zone in the normal direction is

$$k_n(\max) = k_s(\max) = 10 \times \max\left[\frac{K + \frac{4}{3}G}{(\Delta Z)_{\min}}\right] \quad (2)$$

where parameters K and G=bulk and shear moduli, respectively; and $(\Delta z)_{\min}$=smallest dimension of continuum zone adjacent to the interface in normal direction. This approach was used to estimate preliminary values for interface stiffness components, and then these values were adjusted by refining the magnitude of k_n and k_s to avoid intrusion of adjacent zones (a numerical effect) and to prevent excessive computation time. Table 2 summarizes the values for the interface stiffness properties used in the foundation simulations after adjustment from values calculated with Eq. (2). The final stiffness values reported in Table 2 are smaller than the values obtained with Eq. (2) that were used as the starting point in the numerical parametric analyses and in the final simulation runs.

In the numerical model, the value of the shear stiffness of soil–foundation interfaces can be continuously updated, consistent with the changing shear modulus of the adjacent soil column, if a stress-dependent soil model is used. However, the values of soil–foundation interface stiffness parameters k_n and k_s were controlled by the relatively large magnitude of the elastic modulus properties of the facing foundation, compared with the soil elastic modulus [Eq. (2)], and hence these values were constant during simulation runs. The maximum interface shear resistance between the foundation and the soil is controlled by the peak soil cohesion, and a reduced value of the soil cohesion was used for this interface (i.e., c_{sf}=30 kPa in Table 2). A value of k_s=5 MPa/m was selected for soft clay after a number of values were investigated to find a good fit with measured structural deformations and Simultancously avoiding numerical effects such as intrusion of adjacent zones and excessive computation time. Smaller values were found to give excessively large predictions of structure lateral deformations, whereas the magnitude of structure deformations was relatively insensitive to values greater than 5 MPa/m.

Numerical Model Verification

Representative simulation results of the western Canada earthquake high (WCM) ($a_{\max}$=0.18g) event at different depths are shown in Fig. 4, in terms of acceleration time histories and the corresponding response spectra (5% damping) along the soil profile. The results show that the calculated response is in good agreement with the experimental counterpart at all accelerometer locations, both in the time and frequency domains. This confirms that the overall damping of the model (hysteretic plus Rayleigh) represented the experimental damping behavior. Similar to the observed behavior in experiments, the computed response indicated that the seismic waves were amplified as they propagated from the bedrock to the surface. However, the calculated response spectra for periods ranging from 0.2 to 0.5 s were slightly less than the measured response spectra, for the region close to surface in both free field and underneath the structure. This may be attributed to the approximate modeling of the rigid boundaries (i.e., container) around the soil mass, the foundation–soil interface, and material properties of the soil and structure.

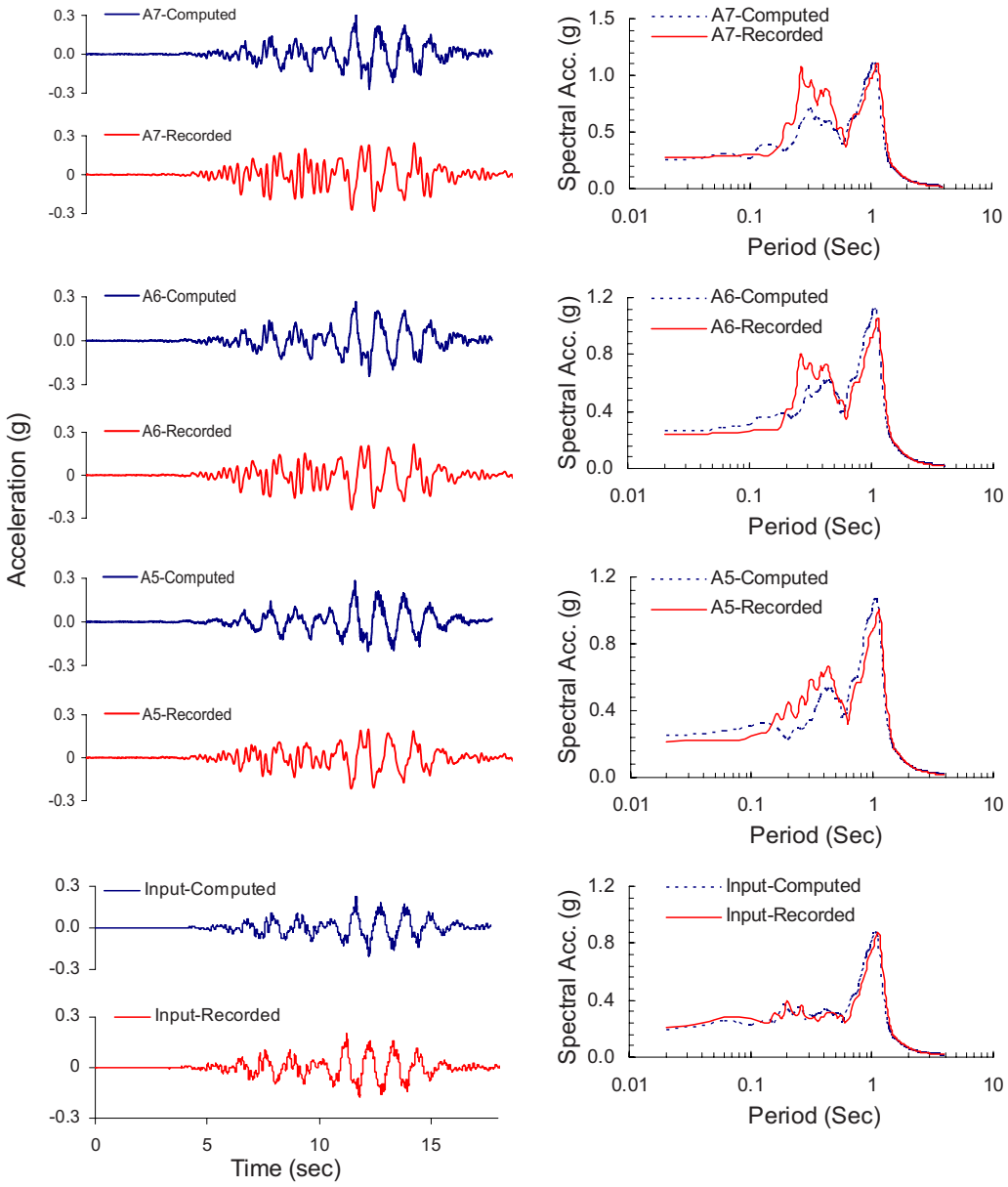

Fig. 4. Comparison between measured and predicted free-field and underneath structure accelerations and response spectra of Model RG-01

Numerical Results and Analyses

The characteristics of the earthquake motion at the base of a structure are affected by the properties of the underlying soil through soil amplification and soil–structure interaction phenomena. A parametric study is performed to evaluate the effects of these phenomena on the free-field motion and the foundation input motion. The parametric study considered different soil profiles and different types of earthquake input motions. The results are presented in terms of peak acceleration, response spectra, and amplification factors.

Amplification of Motion in Soft Soil

The factors that contribute to soft soil amplification include: thickness of soil profile, shear wave velocity-depth function, and seismic wave attenuation. In some circumstances, these factors can yield a combined effect of velocity-gradient amplification and resonance amplification. The vertically aligned acceleration data from the model were used to study the amplification of ground motion in soft soil. Fig. 5 depicts the free-field acceleration amplification for all shaking events. The acceleration of the free field was amplified, with larger amplification occurring for the weaker earthquake excitations. The amplification factor decreased to about 1.12 for stronger shaking events [Kobe earthquake high (KH), $a_{max}=0.54g$].

As was discussed earlier, the material damping of glyben is higher than that of natural clays. Thus, additional viscous (Rayleigh) damping of 10% was employed in addition to the hysteretic damping. In order to estimate the soil amplification in natural soft soils, a series of nonlinear analyses was performed using the hysteretic damping and the relationship proposed by Vucetic and Dobry (1991) for soft clay. As can be noted from Fig. 5, the amplification factor in natural clay is about 10–20% higher than those recorded for the glyben clay, which demonstrates that site effects in soft soil could be even higher than those measured in the current centrifuge tests.

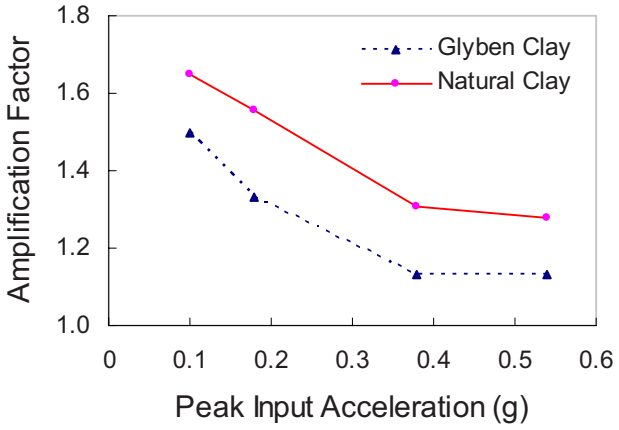

Fig. 5. Free-field soil amplification in glyben and natural soft clay

Effect of Thickness of Soil Profile on Ground Motion

Soil models with different depths were analyzed to investigate the effect of thickness of soil profile on ground input motion. Fig. 6 shows the peak acceleration and period for different earthquake input motions. The input acceleration amplified from the base to the surface, as the soil depth increased from 10 to 70 m. In general, the amplification increased with depth, with the amplification for the first 30 m more significant than for deeper soil profiles. Therefore, considering the properties of the top 30 m of soft soil profiles, as stipulated in most modern codes, would be appropriate for seismic site response analyses in terms of peak ground motion. Meanwhile, the peak spectral acceleration moved toward longer periods as the soil depth increased for all shaking events.

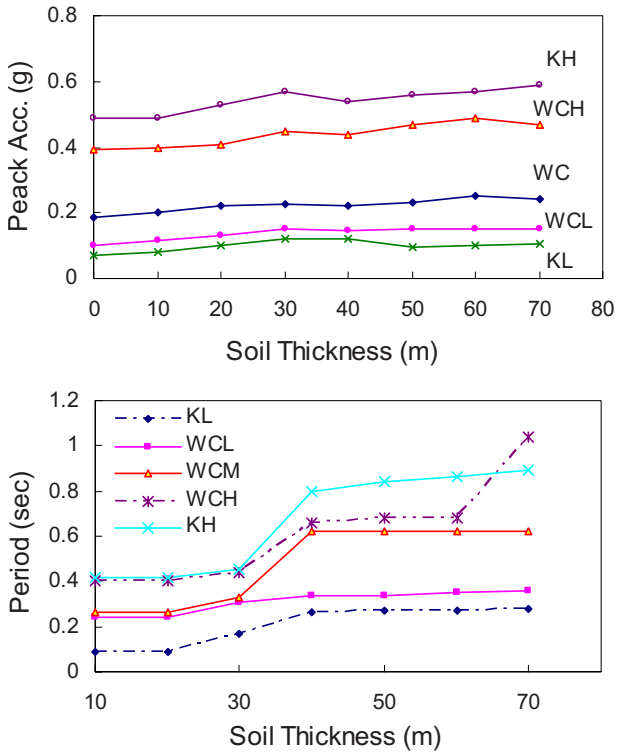

Fig. 6. Peak acceleration and period for different earthquake motions

Table 3. Peak Ground Motion for Different Soil Strata during WCM Event ($a_{max}=0.18g$)

Soil profile	Depth (m)	V_s[a] (m/s)	Average V_s (m/s)	Peak acceleration (g)	Amplification factor
Lay-E0	30	166	166	0.23	1.28
Lay-E1	10	100	166	0.275	1.53
	20	250			
	10	250			
Lay-E2	10	100	166	0.245	1.36
	10	250			
Lay-D0	30	270	270	0.225	1.25
Lay-D1	10	150	270	0.265	1.47
	20	450			
	10	450			
Lay-D2	10	150	270	0.215	1.19
	10	450			

[a]Note: V_s=shear wave velocity.

Effect of Soil Layering on Ground Motion

The average shear wave velocity of the top 30 m in site characterization is recommended in most building codes' seismic provisions. However, ground failure observations during the Northridge Earthquake of 1994, summarized by Holzer et al. (1999), showed that the localized patch in soil strata affected the overall dynamic response of the ground. In order to investigate the effects of soil layering on foundation input motion, a series of analyses was performed on various soil strata categorized in Groups D ($180<V_s<350$ m/s) and E ($V_s<180$ m/s) of Canadian National Building Code provisions (NBCC) in 2005.

Table 3 shows the amplification factor for three soil profiles that can be categorized in Group E of National Building Code of Canada (NBCC) in 2005 based on the average shear wave velocity ($V_s=166$ m/s) and three profiles that can be categorized in Group D ($V_s=270$ m/s). It is noted from Table 3 that the amplification factor varied between 1.28 and 1.53 for Group E profiles and between 1.25 and 1.47 for Group D profiles. It is also noted that the amplification for soil profiles with an upper soft layer is higher than that of the uniform soil profile in both soil categories. These observations demonstrate the importance of considering the soil layering when evaluating the foundation input motion and not just the average of shear wave velocity in the top 30 m of the soil profile.

In case of soft soil trapped between stiff layers, the surface motion could show less amplification compared with uniform soil strata with the same average shear wave velocities (as noted for Soil Group D). Such behavior was reported by Tokimatsu et al. (1996) in the Kobe Earthquake, which demonstrated that local site effects including those resulting from soil liquefaction were responsible for reducing the damage to superstructures particularly located near coast lines.

Effect of SSI on Foundation Input Motion

The effect of kinematic SSI on foundation input motion is assessed by comparing the acceleration amplification underneath the structure with the free-field response. As shown in Fig. 7, the maximum acceleration amplification underneath the structure was higher than that for free field, which indicates the effect of soil–structure interaction. The SSI resulted in amplifying the

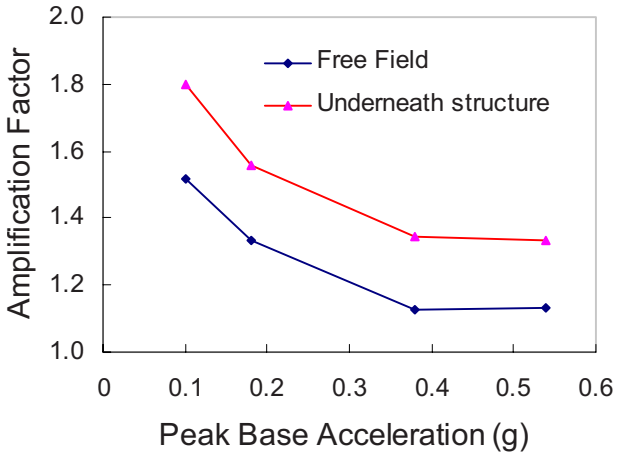

Fig. 7. Effect of SSI on foundation input motion

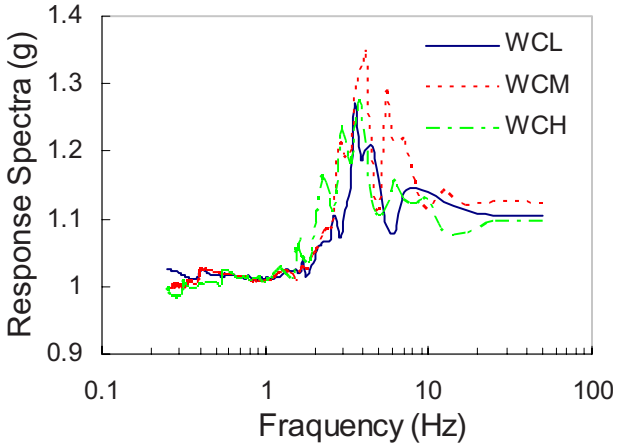

Fig. 9. Response spectral ration of structural wall and beside the structure

ground motion by 15–20% of the maximum accelerations in soft clay. This is qualitatively similar to estimated soil–structure interaction effects which have been identified by Aviles and Perez-Rocha (1997) for medium- and long-period structures located on soft soils in Mexico City during the Mexico earthquake of 1985.

The deviation of the foundation input motion (FIM) from the free-field motion is dependent on the stiffness and geometry of the foundation and soil properties. This deviation is expressed by a transfer function that represents the ratio of foundation and free-field motions in the frequency domain. Fig. 8 shows the response spectra ratio of underneath the structure to the free field ($SA_{FIM}/SA_{free\ field}$). As noted from Fig. 8, the foundation accelerations are up to 37% higher than the free field over the frequency range of 2–6 Hz. These differences are most pronounced for the WCL ($a_{max}=0.1g$) and WCM ($a_{max}=0.18g$) shaking events. The difference between the free-field ground motion and the foundation input motion (in the same level) is not so significant at frequencies less than 2 Hz (5–7%). The parametric analyses indicated that the seismic soil–structure interaction has unfavorable effects on horizontal ground motions for frequencies between 2 and 6 Hz.

The inertial soil–structure interaction was evaluated by comparing the acceleration response spectra of the structure wall with those beside the foundation. Fig. 9 shows the ratio of response spectra of the structure to the response beside the structure in foundation level. It is noted that the structure experienced higher acceleration up to 34% compared to the response beside the foundation level over the frequency range of 3–5 Hz. This higher response indicates the effect of inertial SSI on structural behavior.

An analysis series was also performed on fixed-base structure and its response was compared with response of the structure on different soil profiles to evaluate the effect of SSI (both kinematic and inertial) on structural response. As can be seen from Fig. 10, SSI amplified the fixed-base structural response from 0.3*g* up to 1.6*g* in soft soil. Soil–structure interaction also increased the natural period of the fixed-base structure from 0.15 s to about 0.3 s.

The relationship among the vibration frequencies of the model structure, natural frequency of the supporting soil, and predominant frequency of earthquake input motion influences the seismic response of structures. The natural frequency and stiffness of the building for both soil models are shown in Table 4 for different shaking events. The natural frequency of the soil is close to the vibration frequency of the structure, resulting in significant amplification of input motion. However, the predominant frequency of input motion is lower than the natural frequencies of soil and structure.

Effect of Boundary Condition on FIM

The effect of model container size and type on the model response is an important concern in physical model tests. The

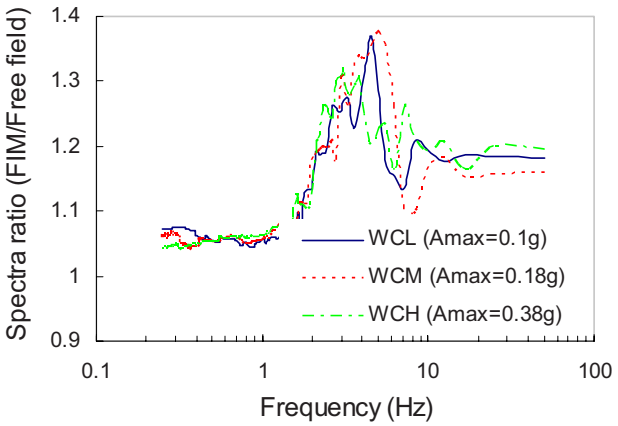

Fig. 8. Spectral ratio ($SA_{FIM}/SA_{free\ field}$) for three shaking events

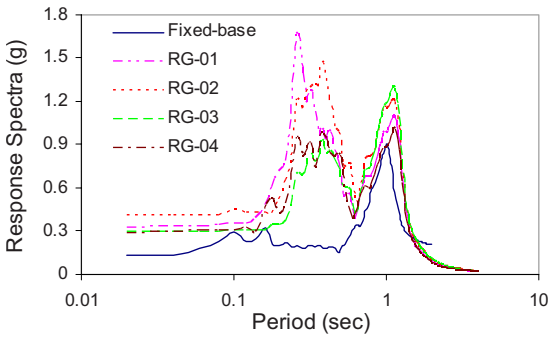

Fig. 10. Response spectra of fixed-base structure and structure on different soil profile

Table 4. Stiffness and Natural Period of the Model Structure

Model event	Soil description	Stiffness, K_u (N/m)			Natural frequency (Hz)		
		WCL	WCM	WCH	WCL	WCM	WCH
RG-01	Uniform	1.23×10^8	1.1×10^8	5.9×10^7	3.5	3.2	2.5
RG-02	Layered	1.64×10^8	1.45×10^8	8.68×10^7	4.0	3.5	3.0

boundary conditions should ideally represent actual field situations with reasonable accuracy. The effect of the distance from the boundary (rigid container wall) to the foundation on the seismic response of Models RG-01 and RG-02 was studied numerically. The boundary in both x and y directions was located at a distance $10B$ ($120\times60\times30$ m) and the results are compared with the original boundary conditions, $5B$ ($60\times30\times30$ m). The results shown in Fig. 11 indicate that the larger rigid container slightly reduced the peak acceleration in both free field (level of A6 in Fig. 1) and beneath the structure. The peak acceleration beneath the structure was decreased by about 5%, from $0.27g$ for Model RG-01 with $5B$ to about $0.255g$ in the large model ($10B$) for WCM ($a_{max}=0.18g$) shaking event. This may be attributed to reduction in wave reflection in the larger container (reduced box effect).

Embedment Effect on Seismic SSI

Most foundations do not rest on the surface of the soil but are partly embedded. Embedment is known to increase both stiffness and damping of the foundation system, but the increase in damping is more significant (Novak, 1964). In addition, Halabian and El Naggar (2002) investigated the seismic performance of tall towers with significant embedment. They concluded that the SSI may have a large effect on the base shear of the tower and should be considered in the analysis.

The effect of embedment of the study structure on SSI characteristics was evaluated. Analyses were performed considering both massless structure model and structures with mass to investigate the kinematic SSI and total SSI effects. The response of the structure was analyzed without embedment and with embedment at varying depths under different input motions. The data obtained from the analyses and centrifuge tests were used to evaluate foundation input motions, structural response, and the SSI characteristics of backfill and surrounding soils.

Fig. 12 shows the response spectra of horizontal acceleration time histories obtained through earthquake excitations of the soft clay models during the WCM ($a_{max}=0.18g$) event for massless structure. It is noted that kinematic interaction reduced the amplitude of foundation motions as a result of base embedment effects. These effects are most pronounced at high frequencies (short periods) of excitation. The peak acceleration amplitude decreased from $0.38g$ for nonembedded structure to $0.27g$ for 5 m embedded structure. The difference between the maximum response spectra for nonembedded structure and 3 m embedded structure was more significant than the difference between the 3 and 5 m embedded structures. These results were consistent, in trend, with the theoretical and experimental studies (e.g., Morris 1981; Hushmand 1983).

An analysis series was also performed considering the mass of structure to evaluate the effects of embedment on total SSI characteristics (both kinematic and inertial interaction). As can be seen from Fig. 13, the amplitude of the spectra peaks slightly decreased with embedment due to SSI. The peak response amplitude decreased from 0.29 for nonembedded structure to 0.25 for 5 m embedded structure.

The structure base shear force was also estimated for all embedment cases considering the mass of structure. The maximum horizontal base shear of 1,066 kN for nonembedded structure decreased to about 1,020 kN for 3 m embedded and 1,006 kN for 5 m embedded structure during the WCM ($a_{max}=0.18g$) event. It is, therefore, concluded that the embedment generally leads to a beneficial reduction in structural loads that is accompanied by an increase in energy dissipation.

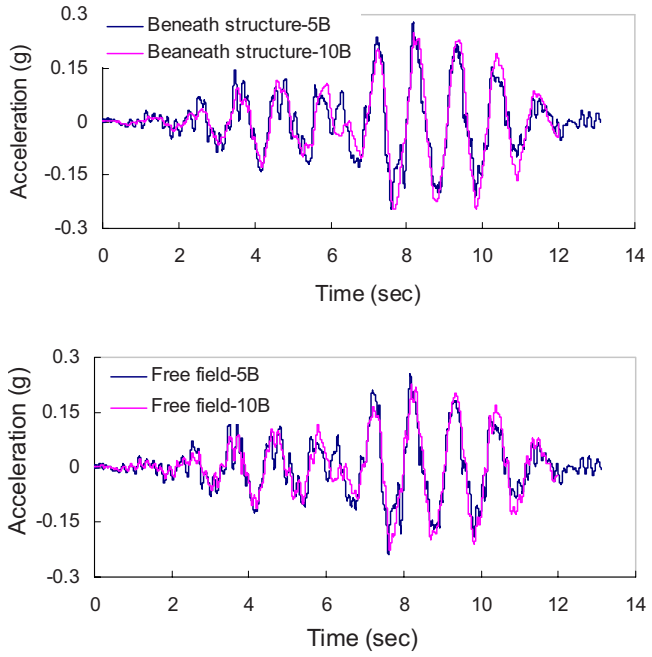

Fig. 11. Effect of location of boundary on acceleration in free field and beneath structure for event WCM ($a_{max}=0.18g$)

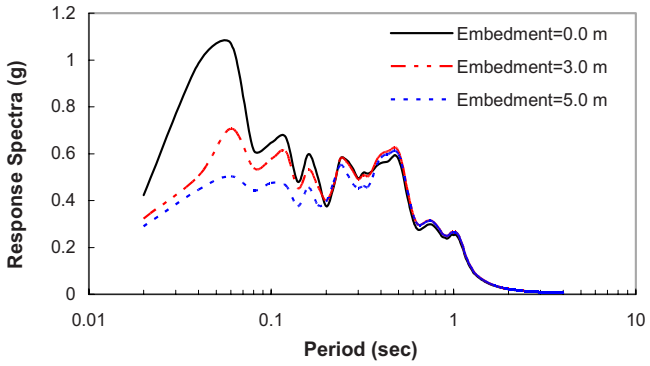

Fig. 12. Response spectra for massless buildings with different embedment during WCM event ($a_{max}=0.18g$)

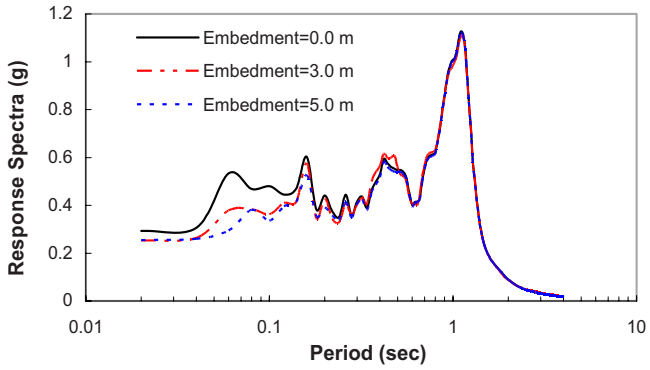

Fig. 13. Response spectra for buildings with mass for different embedment during WCM event (a_{max}=0.18g)

Conclusions

A numerical model was developed using a fully coupled nonlinear finite-difference program (FLAC) to predict the seismic response of a rigid foundation in soft soil. The numerical model was verified/calibrated by comparing its predictions with the measured responses of two centrifuge model tests on uniform and layered clay. The numerical simulations were conducted for a representative set of weak to strong shaking events. The validated model was then used to study the effects of thickness of soil profile and layering on earthquake amplification and soil–structure interaction. In addition, the embedment effects on foundation input motions were investigated. The following conclusions were drawn:

1. The acceleration of the free field was significantly amplified, especially for low earthquake input motions. It was found that most amplification occurred within the first 30 m of the soil profile, which is in agreement with most modern seismic codes that evaluate local site effects based on the properties of the top 30 m of the soil profile. However, the peak spectral acceleration moved toward longer periods as the soil depth increased.
2. Soil layering was found to have a significant effect on ground motion amplification in both Soil Groups D and E as specified by NBCC in 2005. The presence of a top soft layer within the profile can significantly increase the ground motion amplification relative to the case of a uniform soil profile with the same average shear wave velocity of the top 30 m of the soil profile.
3. The peak accelerations of soil beneath the structure increased due to strong interaction between the soil and the foundation. For the case considered, the seismic soil–structure interaction increased the horizontal ground motions at frequencies 2–6 Hz.
4. The results showed that increasing the distance of a rigid boundary from five times the width of the structure to ten times the width has a small effect (5% change) on the seismic response of the models. It may be concluded that placing rigid boundary at a distance equal to five times the width of the structure is acceptable when carrying physical or numerical models for seismic purposes.
5. The embedment of the structure decreased the amplitude of the response spectra significantly.

References

Aviles, J., and Perez-Rocha, L. E. (1997). "Site effects and soil-structure interaction in the valley of Mexico." *Soil Dyn. Earthquake Eng.*, 17, 29–39.

Balenda, T., and Heidebrecht, A. C. (1986). "Influence of different sites on seismic base shear of buildings." *Earthquake Eng. Struct. Dyn.*, 14, 623–642.

Borja, R. I., Chao, H. Y., Montans, H. J., and Lin, C. H. (1999). "SSI effects on ground motion at Lotung LSST Site." *J. Geotech. Geoenviron. Eng.*, 125(9), 760–770.

Crouse, C. B., and Ramirez, J. C. (2003). "Soil-structure interaction and site response at the Jensen Filtration Plant during the 1994 Northridge, California." *Bull. Seismol. Soc. Am.*, 93(2), 546–556.

De Barros, F. C. P., and Luco, J. E. (1995). "Identification of foundation impedance functions and soil properties from vibration tests of the Hualien containment model." *Soil Dyn. Earthquake Eng.*, 14, 229–248.

Elsabee, F., and Morray, J. P. (1977). "Dynamic behavior of embedded foundation." *Rep. No. R77-33*, Dept. of Civil Engineering, Massachusetts Institute of Technology, Cambridge, Mass.

Faccioli, E., Paolucci, R., and Vivero, G. (2001). "Investigation of seismic soil-footing interaction by large scale cyclic tests and analytical models." *4th Int. Conf. on Recent Advances in Geotech. Earthquake Engineering and Soil Dynamics*, 26–31.

Gajan, S., Kutter, B. L., Phalen, J. D., Hutchinson, T. C., and Martin, G. R. (2005). "Centrifuge modeling of load-deformation behavior of rocking shallow foundations." *Soil Dyn. Earthquake Eng.*, 25, 773–783.

Georgiadis, M., and Butterfield, R. (1988). "Displacements of footings on sand under eccentric and inclined loads." *Can. Geotech. J.*, 25, 199–212.

Ghosh, B., and Madabhushi, S. P. G. (2003). "Effect of localized soil inhomogenity in modifying seismic soil structure interaction." *ASCE 16th Engineering Mechanics Conf.*, ASCE, New York, 1–8.

Halabian, A. M., and El Naggar, M. H. (2002). "Effect of foundation flexibility on seismic response of R/C TV-towers." *Can. J. Civ. Eng.*, 28(3), 465–481.

Holzer, T., Bennett, M., and Ponti, D. (1999). "Liquefaction and soil failure during 1994 Northridge Earthquake." *J. Geotech. Geoenviron. Eng.*, 126(6), 438–452.

Hushmand, B. (1983). "Experimental studies of dynamic response of foundations." Ph.D. thesis, California Institute of Technology, Calif.

Itasca Consulting Group, Inc. (Itasca). (2005). *FLAC3D*: "Fast Lagrangian analysis of continua in 3 dimensions, version 3.0." *User's manual*, Minneapolis.

Kim, S. (2001). "Calibration of simple models for seismic soil structure interaction from field performance data." Ph.D. Dissertation, Univ. of California, Los Angeles.

Kim, S., and Roesset, J. M. (2004). "Effect of nonlinear soil behavior on inelastic seismic response of a structure." *Int. J. Geomech.*, 4(2), 104–114.

Kim, S., and Stewart, J. P. (2003). "Kinematic soil-structure interaction from strong motion recordings." *J. Geotech. Geoenviron. Eng.*, 129(4), 323–335.

Lin, A. N., and Jennings, P. C. (1984). "Effect of embedment on foundation-soil impedances." *J. Eng. Mech.*, 110, 1060–1075.

Luco, J. E., and Mita, A. (1987). "Response of circular foundation to spatially random ground motions." *J. Eng. Mech.*, 113(1), 1–15.

Luco, J. E., Trifunac, M. D., and Wong, H. L. (1988). "Isolation of soil-structure interaction effects by full-scale forced vibration tests." *Earthquake Eng. Struct. Dyn.*, 16, 1–21.

Luco, J. E., and Wong, H. L. (1986). "Response of a rigid foundation to a spatially random ground motions." *J. Eng. Mech.*, 113(2), 1–15.

Morris, D. V. (1981). "Dynamic soil-structure interaction modeled experimentally on a geotechnical centrifuge." *Can. Geotech. J.*, 18(1), 40–51.

Novak, M. (1964). "Effect of soil on structural response to wind and

earthquake." *Earthquake Eng. Struct. Dyn.*, 3(1), 79–96.
Randolph, M. F., and Houlsby, G. T. (1984). "The limiting pressure on a circle pile loaded laterally in cohesive soil." *Geotechnique*, 34(4), 613–623.
Rayhani, M. H. T., and El Naggar, M. H. (2007). "Centrifuge modeling of seismic response of layered soft clay." *Bull. Earthquake Eng.*, 5(4), 571–589.
Rayhani, M. H. T., and El Naggar, M. H. (2008). "Characterization of glyben for seismic application." *Geotech. Test. J.*, 31(1), 24–31.
Stewart, J. P., Kim, S., Bielak, J., Dobry, R., and Power, M. S. (2003). "Revisions to soil-structure interaction procedures in NEHRP design provisions." *Earthquake Spectra*, 19(3), 677–696.
Tokimatsu, K., Mizuno, H., and Kakurai, M. (1996). "Building damage associated with geotechnical problems." *Soils Found.*, Jan., 219–234.
Veletsos, A. S., and Prasad, A. M. (1989). "Seismic interaction of structures and soils: Stochastic approach." *J. Struct. Eng.*, 115(4), 935–956.
Veletsos, A. S., Prasad, A. M., and Wu, W. H. (1997). "Transfer functions for rigid rectangular foundations." *Earthquake Eng. Struct. Dyn.*, 26, 5–17.
Vucetic, M., and Dobry, R. (1991). "Effect of soil plasticity on cyclic response." *J. Geotech. Engrg.*, 117(1), 89–107.
Wiessing, P. R. (1979). "Foundation rocking on sand." Master's thesis, *School of Engineering Rep. No. 203*, Univ. of Auckland, Auckland, Australia.